

See discussions, stats, and author profiles for this publication at: <https://www.researchgate.net/publication/6838204>

# Formation of Parallel Strips in Thin Films of Polystyrene/Poly(vinyl pyrrolidone) Blends via Spin Coating on Unpatterned Substrates

ARTICLE *in* LANGMUIR · OCTOBER 2006

Impact Factor: 4.46 · DOI: 10.1021/la060418w · Source: PubMed

---

CITATIONS

23

---

READS

11

3 AUTHORS, INCLUDING:



Shih-Yuan Lu

National Tsing Hua University

159 PUBLICATIONS 3,070 CITATIONS

SEE PROFILE

# Formation of Parallel Strips in Thin Films of Polystyrene/Poly(vinyl pyrrolidone) Blends via Spin Coating on Unpatterned Substrates

Kuen-Hua Wu, Shih-Yuan Lu,\* and Hsin-Lung Chen

Department of Chemical Engineering, National Tsing-Hua University, Hsin-Chu 30043, Taiwan, R.O.C.

Received February 13, 2006. In Final Form: May 16, 2006

Patterns of parallel strips, consisting of alternating polystyrene (PS) and poly(vinyl pyrrolidone) (PVP) regions, were observed in thin films spin cast from a PS/PVP/chloroform solution on unpatterned substrates. The formation of anisotropic patterns, manifested not only in thickness variation but also in composition variation, was found to be driven by Marangoni instability, with the PS and PVP streams flowing toward the preferred regions as the phase separation induced by solvent evaporation proceeded. The initial viscosity of the polymer solution and the thickness of the spin-cast films were lumped into one single parameter to study the phase morphology development at various initial polymer solution concentrations. Interestingly, the ratio of the square of the film thickness to the viscosity, a parameter loosely related to the Marangoni number, was found to reach a maximum value at the concentration where the strip patterns were most well-developed.

## Introduction

Phase separation of polymer blends in bulk has been extensively studied over the past few decades. The demixing process commonly leads to an *isotropic* and *disordered* morphology of the coexisting phases. As for thin films of polymer blends, because of the large surface-to-volume ratio, the structure of the separating phases is different from that in the bulk.<sup>1–5</sup> The thin films of polymer blends have found potential applications in biomaterials<sup>6</sup> and optoelectronics.<sup>7</sup> In particular, the low cost of polymer pattern formation can be an integral part in the development of all-polymer semiconductor devices, such as integrated circuits and display elements.<sup>8</sup>

On the surface of the spin-cast films, the so-called radiative striations, which are radially extended ridges, are often observed.<sup>9</sup> This phenomenon occurs particularly when the polymer films are spin cast from highly volatile solvents, which induces a strong Marangoni effect.<sup>10,11</sup> The rapid solvent evaporation near the solution surface leads to nonuniform composition and temperature gradients and thus drives the convective flows. The occurrence of the instability is mainly governed by the interplay among surface tension, diffusion, and viscosity, which can be characterized by the Marangoni number,  $Ma$ :<sup>12</sup>

$$Ma = \frac{-(\partial\gamma/\partial T)H^2\nabla T}{\mu\alpha} \quad (1)$$

or

$$Ma = \frac{-(\partial\gamma/\partial C)H^2\nabla C}{\mu D} \quad (2)$$

where  $(\partial\gamma/\partial T)$  is the temperature derivative of the surface tension,  $\nabla T$  is the temperature gradient near the solution surface,  $(\partial\gamma/\partial C)$  is the concentration derivative of the surface tension,  $\nabla C$  is the concentration gradient near the solution surface,  $H$  is the film thickness,  $D$  is the mass diffusivity of the component, and  $\mu$  and  $\alpha$  are the viscosity and thermal diffusivity of the solution, respectively. Equation 1 applies for the case where the temperature gradient dominates the Marangoni effect, whereas eq 2 applies when the concentration gradient is the main driving force. The critical value of  $Ma$ , above which the instability is triggered, is around 80. For spin-coating processes, the film thickness may not be sufficiently large to give a high enough  $Ma$  value for inducing the stable thermocapillary convection according to the above equation. Nevertheless, Birnie et al.<sup>13</sup> pointed out that the solutocapillary flow induced by concentration gradients is more important than the thermocapillary flow caused by temperature gradients.

Muller-Buschbaum et al.<sup>14</sup> showed the formation of striation patterns over a spin-cast polystyrene (PS) film and correlated the surface morphology with the vapor pressure of the solvents. When using solvents of low vapor pressures, the resulting films were homogeneous. If solvents of intermediate vapor pressure were used, marked striation characterized by periodic variation in surface thickness was observed. Smoother films appeared again with solvents of high vapor pressures. Kumar et al.<sup>15</sup> showed the cellular morphology of spin-cast films of PS and poly(ethyl methacrylate). Yamamura et al.<sup>16</sup> demonstrated that the introduction of a temperature gradient along the free surface induced a particular strip pattern in phase-separating fluids. The horizontal temperature gradient drove laterally periodical spiral liquid motion

\* Corresponding author. Fax: +886-3-5715408. Tel: +886-3-5714364. E-mail: sylu@mx.nthu.edu.tw.

(1) Walheim, S.; Boltau, M.; Mlynek, J.; Krausch, G.; Steiner, U. *Macromolecules* **1997**, *30*, 4995.

(2) Karim, A.; Slawicki, T. M.; Kumar, S. K.; Douglas, J. F.; Satija, S. K.; Han, C. C.; Russell, T. P.; Liu, Y.; Overney, R.; Sokolov, J.; Rafailovich, M. *Macromolecules* **1998**, *31*, 857.

(3) Walheim, S.; Ramstein, M.; Steiner, U. *Langmuir* **1999**, *15*, 4828.

(4) Wang, H.; Composto, R. J. *Macromolecules* **2002**, *35*, 2799.

(5) Liao, Y.; Su, Z.; Ye, X.; Li, Y.; You, J.; Shi, T.; An, L. *Macromolecules* **2005**, *38*, 211.

(6) Granick, S.; Kumar, S. K.; Amis, E. J.; Anionietti, M.; Balazs, A. C.; Chakraborty, A. K.; Grest, G. S.; Hawker, G.; Janmey, P.; Kramer, E. J.; Nuzzo, R.; Russell, T. P.; Safinya, C. R. *J. Polym. Sci., Part B* **2003**, *41*, 2755.

(7) Luo, S. C.; Craciun, V.; Douglas, E. P. *Langmuir* **2005**, *21*, 2881.

(8) Sprenger, M.; Walheim, S.; Schafle, C.; Steiner, U. *Adv. Mater.* **2003**, *15*, 703.

(9) Du, X. M.; Orignac, X.; Almeida, R. M. *J. Am. Ceram. Soc.* **1995**, *78*, 2254.

(10) Scriven, L. E.; Sterling, C. V. *Nature* **1960**, *187*, 186.

(11) Pearson, J. R. A. *Fluid Mech.* **1958**, *4*, 489.

(12) Haas, D. E.; Birnie, D. P. *J. Mater. Sci.* **2002**, *37*, 2109.

(13) Birnie, D. P. *J. Mater. Res.* **2001**, *16*, 1145.

(14) Muller-Buschbaum, P.; Gutmann, J. S.; Wolkenhauer, M.; Kraus, J.; Stamm, M.; Smilgies, D.; Petry, W. *Macromolecules* **2001**, *34*, 1369.

(15) Strawhecker, K. E.; Kumar, S. K.; Douglas, J. F.; Karim, A. *Macromolecules* **2001**, *34*, 4669.

(16) Yamamura, M.; Nakamura, S.; Kajiwara, T.; Kage, H.; Adachi, K. *Polymer* **2003**, *44*, 4699.

**Table 1. Characteristics of Polymers and Solvent Used in This Work**

materials	$M_n$	$\mu$ (cps) at 1.3% chloroform solution	$\gamma_s$ observed (mJ/m <sup>2</sup> )	$\rho$ (g/cm <sup>3</sup> )	$\gamma_s$ calculated (mJ/m <sup>2</sup> )
PS-1	176 000	2.9	43 <sup>a</sup>	1.08 <sup>b</sup>	42 <sup>d</sup>
PS-2	45 000	0.9			
PVP	69 000	1.2	NA	1.2 <sup>c</sup>	56 <sup>d</sup>
chloroform		0.7	29	1.48	

<sup>a</sup> See ref 28. <sup>b</sup> See ref 29. <sup>c</sup> See ref 30. <sup>d</sup> The surface tension was estimated from  $\gamma_s = (\text{Ps}/V)^4$ , where Ps and V are the Parachor value and the molar volume, respectively.<sup>31</sup>

flowing from warmer to cooler regions due to thermocapillarity. Kumacheva et al.<sup>17,18</sup> presented studies on surface-tension-driven convection in thin layers of poly(dimethyl siloxane) oligomers and PS/poly(methyl methacrylate) blends, where the resulting solvent-cast films exhibited ordered hexagonal patterns.

In the present study, we demonstrate the formation of periodic strips in thin films of PS/poly(vinyl pyrrolidone) (PVP) blends on unpatterned substrates via spin coating. The morphological evolution of spin-cast polymer blend films has been investigated extensively.<sup>1,19–27</sup> However, most of the studies obtained only isotropic, irregular patterns, which were well-known and commonly encountered in polymer phase-separation processes (e.g., spinodal decomposition), except for studies in which the substrates were patterned with self-assembled monolayer microcontact printing or were corrugated prior to the spin coating. In this case, the resulting periodic strips were replicated from the patterns on the substrates.<sup>25–27</sup> The present work is the first to report ordered, self-organized, *anisotropic* patterns (striations) on *unpatterned* substrates. We propose a possible formation mechanism for the strip patterns and show that the mechanism is relevant to the Marangoni instability. The relevant variables, which may affect the morphological evolution, were also discussed.

### Experimental Section

**Materials.** PS (PS-1, PS-2) and PVP were purchased from Scientific Polymer and Acros, respectively. PS/PVP blends were prepared by dissolving the polymers in chloroform at concentrations of 0.6–5.0 wt %. The blend compositions reported in this study are all in weight percent. The characteristics of the materials used are summarized in Table 1. The surface tension of the solvent is smaller than those of the two polymers, and the vapor pressure of the solvent is high, giving a fast solvent evaporation. These are the key factors to trigger Marangoni instability.

**Surface Treatment of Substrates.** Glass slides (2.5 × 2.5 cm) were used as the substrates for the spin-coating process. The surfaces of the glass slides were treated with two different procedures to

obtain either hydrophilic or hydrophobic substrates. Hydrophilic substrates were prepared by simply cleaning the glass slides with a H<sub>2</sub>SO<sub>4</sub>/H<sub>2</sub>O<sub>2</sub> (piranha) mixture to remove the organic residues. To produce hydrophobic substrates, the piranha-cleaned glass slides were immersed overnight in a 6% (w/w) solution of trimethylchlorosilane (TMCS) in hexane. The static water contact angles of the two treated substrates were <10° and 91–100° for piranha-cleaned and TMCS-modified glass slides, respectively.

**Preparation and Characterization of Blend Thin Films.** A 90  $\mu$ L portion of a PS/PVP/chloroform blend solution was dropped onto the glass substrate followed by spinning at controlled rotation speeds for 30 s to make the thin films of PS/PVP blends. The morphological patterns were well-developed right after the film formation.

The real-space morphology of the blend films was observed with an Olympus BH2-UWA optical microscope (OM) in transmission mode. The static light-scattering patterns were obtained with a 20 mW He–Ne laser (wavelength of 633 nm). The film thickness and the blend solution viscosity were measured with an  $\alpha$ -step surface profiler and a cone-and-plate viscometer, respectively. Synchrotron radiation–Fourier transform infrared microscopy (micro-SR–FTIR), with an aperture size of 10 × 10  $\mu$ m, was conducted to obtain infrared absorption spectra of the selected areas on the blend thin film. The surface topography of the blend thin films was characterized with a NanoScope E atomic force microscope (AFM) in contact mode.

### Results and Discussion

Prior to the study of the PS/PVP blend films, the thin films of neat PS-1, PS-2, and PVP were prepared by spin coating on the glass substrates (piranha-cleaned and TMCS-modified) to reveal the morphology of the corresponding homopolymer thin films. Three different solution concentrations (0.9, 1.3, and 2.5%) were used to prepare the spin-cast films at a rotation speed of 6000 rpm. All the resulting thin films showed periodic thickness variation at the film surface, as shown in Figure 1a for the PS-1 film, only the degree of thickness variation of each sample was not the same. This type of pattern is called striation, induced by Marangoni instability and previously observed for other homopolymers. However, the factors affecting the morphological development of spin-cast films are complex; even the air flow above the films is important. Therefore, the detailed mechanism underlying the formation of the regularity of striations is still unclear.

**Characterizations of Blend Thin Films Spin Cast on Hydrophilic Substrates. Morphology Evolution at Different Blend Compositions.** Shown in Figure 1b–e are the morphologies of thin films of PS-1/PVP blends spin cast at 6000 rpm using a solution concentration of 1.3%. The formation of a phase-separated morphology under the influence of Marangoni instability is evident. At the 10/90 composition, the minor PS domains showed up as discrete disks, lining up along the radial direction with rather uniform spacing between the lines (Figure 1b). Apparently, the amount of PS was not enough to form continuous lines here. As the amount of PS increased to 20 wt %, most disks interconnected to form continuous strips, while some still remained dispersed between the strips (Figure 1c). When the PS content was further increased to 30 wt %, the strip width increased, with those disks trapped between the strips forming larger domains. Branching of the strips also started to occur here (Figure 1d). At the 40/60 composition, the parallel strips grew even thicker with more branches. The trapped domains not only became larger, but also connected to the strips forming a bush-like structure.

The chemical compositions of the separated phases, namely, the strips and the region between the strips, in the films were probed with micro-FTIR. Figure 2a shows the real-space

- (17) Mitov, Z.; Kumacheva, E. *Phys. Rev. Lett.* **1998**, *81*, 3427.
- (18) Li, M.; Xu, S.; Kumacheva, E. *Macromolecules* **2000**, *33*, 4972.
- (19) Dekeyser, C. M.; Biltresse, S.; Marchand-Brynaer, J.; Rouxhet, P. G.; Dupont-Gillain, C. C. *Polymer* **2004**, *45*, 2211.
- (20) Tanaka, K.; Takahara, A.; Kajiyama, T. *Macromolecules* **1996**, *29*, 3232.
- (21) Kang, H.; Lee, S. H.; Kim, S.; Char, K. *Macromolecules* **2003**, *36*, 8579.
- (22) Prosycevas, I.; Tamulevicius, S.; Guobiene, A. *Thin Solid Films* **2004**, *453–454*, 304.
- (23) Wang, P.; Koberstein, J. T. *Macromolecules* **2004**, *37*, 5671.
- (24) Heriot, S.; Jones, R. *Nat. Mater.* **2005**, *4*, 782.
- (25) Boltau, M.; Walheim, S.; Mlynek, J.; Krausch, G.; Steiner, U. *Nature* **1998**, *391*, 877.
- (26) Li, X.; Xing, R.; Zhang, Y.; Han, Y.; An, L. *Polymer* **2004**, *45*, 1637.
- (27) Geoghegan, M.; Krausch, G. *Prog. Polym. Sci.* **2003**, *28*, 261.
- (28) Lee, V. A.; Craig, R. G.; Filisko, F. E.; Zand, R. *J. Biomed. Mater. Res.* **1996**, *31*, 51.
- (29) Coskun, M.; Demirelli, K.; Oezdemir, E. *Polym. Degrad. Stab.* **1995**, *47*, 251.
- (30) Matsumoto, T.; Zograf, G. *Pharm. Res.* **1999**, *16*, 1722.
- (31) Van Krevelen, D. W. In *Properties of Polymers*, 3rd ed.; Elsevier: Amsterdam, 1990; p 229.

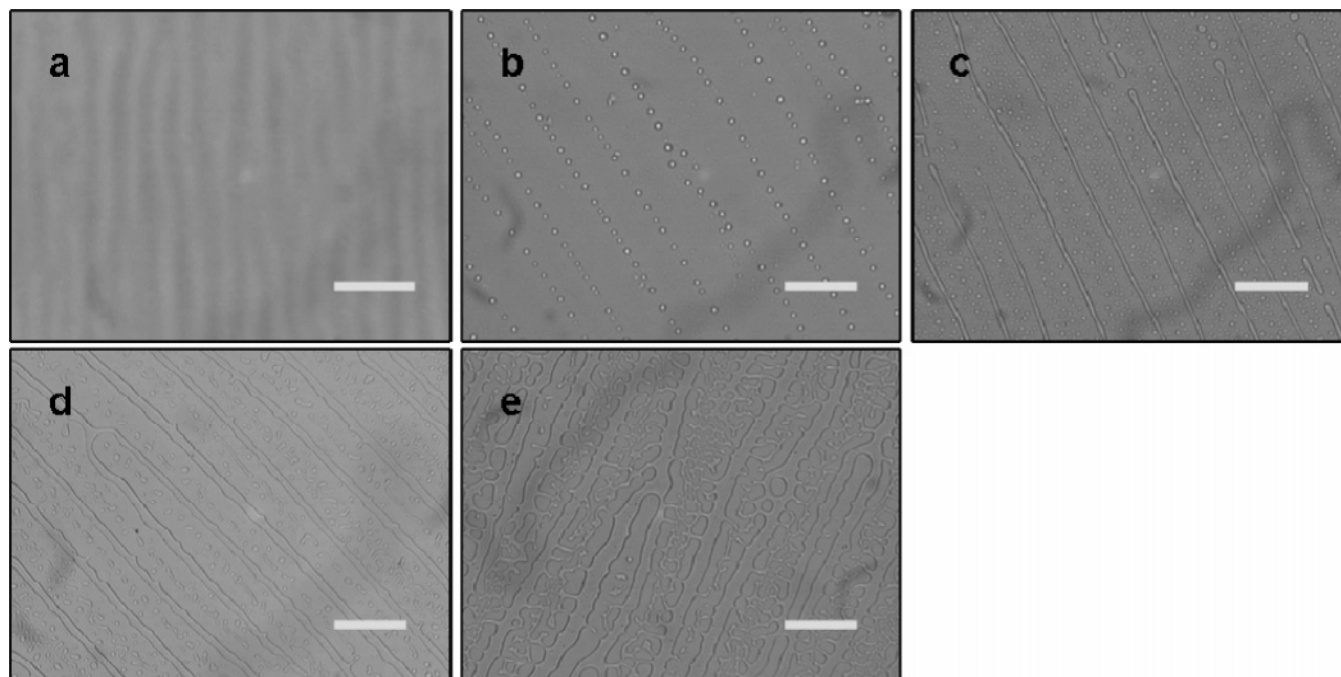


**Figure 1.** OM images of polymer thin films spin cast on hydrophilic glass substrates using a solution concentration of 1.3% at 6000 rpm: (a) PS-1, (b) PS-1/PVP = 10/90, (c) PS-1/PVP = 20/80, (d) PS-1/PVP = 30/70, (e) PS-1/PVP = 40/60. The scale bars represent a length of 100  $\mu\text{m}$  in panel a and 50  $\mu\text{m}$  in panels b–e.

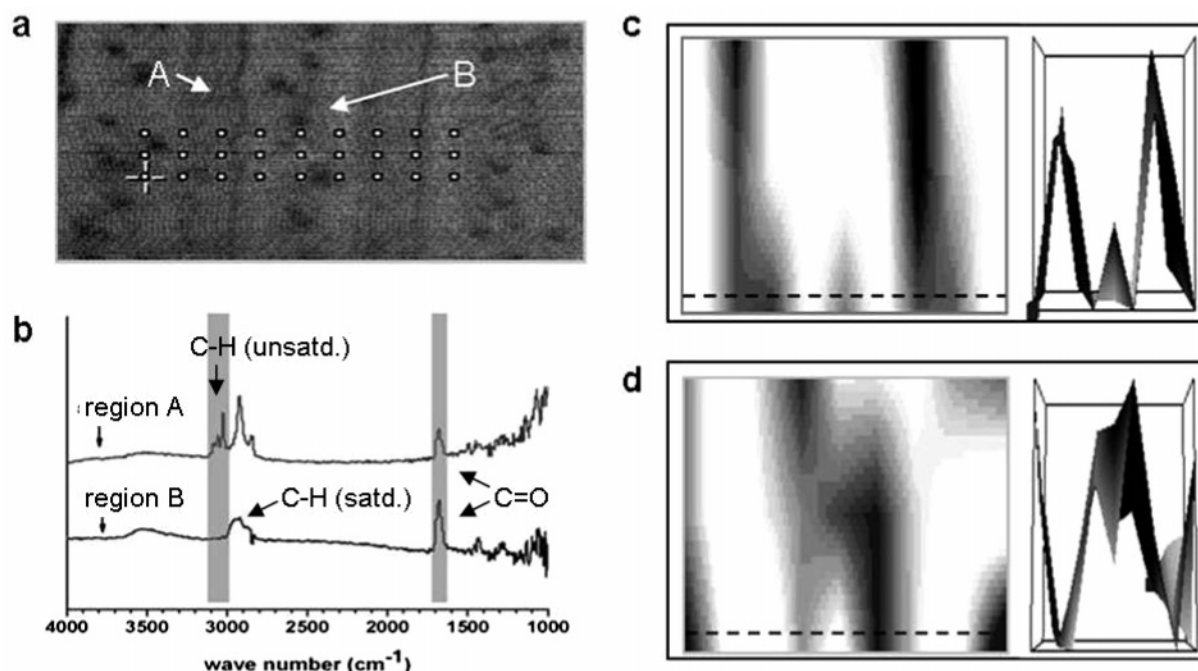


**Figure 2.** Composition of separated phases in a PS-1/PVP (30/70) blend film probed with micro-SR-FTIR: (a) the real-space morphology of the blend film observed under visible light; (b) the absorption spectra obtained from regions A and B indicated in panel a; (c,d) the absorption images associated with unsaturated C–H stretching and C=O stretching, respectively. The region under analysis was a  $9 \times 3$  array shown in panel a. The darker region in the image corresponds to the region with stronger absorption. The cross-sectional intensity profiles along the dashed lines are shown on the right of the absorption images.

morphology of the 30/70 blend film observed under visible light with the focus and brightness adjusted for infrared analysis. Figure 2b displays the IR absorption spectra from regions A and B indicated in Figure 2a. The infrared beam size was set as small as  $10 \times 10 \mu\text{m}$ . The absorption bands corresponding to the saturated and unsaturated C–H stretching are located below and above  $3000 \text{ cm}^{-1}$ , respectively. The unsaturated C–H absorption resulting from the benzene ring in PS was identified in the spectrum of region A, while the C=O stretching associated with

PVP was observed for both regions A and B, but the intensity was much lower for region B. The broad absorption at around  $3600 \text{ cm}^{-1}$  was due to the O–H stretching; however, since neither PS nor PVP possess the OH group, the OH absorption may arise from the moisture absorbed by the hygroscopic PVP. The IR spectra of regions A and B clearly revealed that the corresponding composition was predominately PS and PVP, respectively. Because of the comparable sizes of the infrared beam and the strips, the beam directed to region A may cover a minor portion



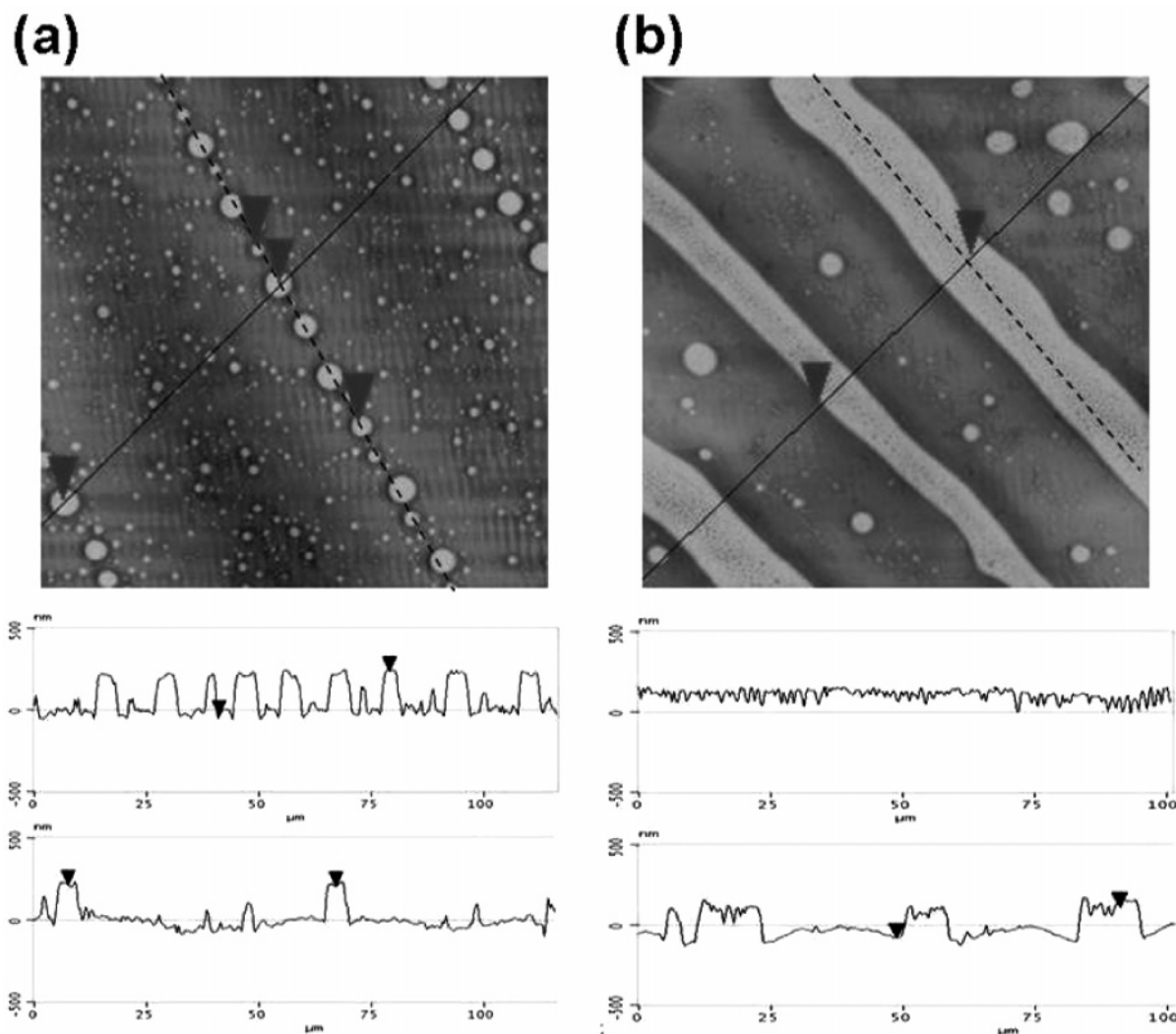


**Figure 3.** AFM topographic images and sectional views along the dashed and solid lines in the AFM images for spin-coated blend films with compositions of (a) 10/90 and (b) 30/70.

of region B, leading to the weak C=O absorption in spectrum A. We have also obtained the images associated with specific absorption bands by scanning the  $9 \times 3$  array specified in the real-space image (Figure 2a). The images shown in Figure 2c,d correspond to the unsaturated C–H and C=O stretching mapping, respectively, with the darker region representing the stronger absorption. Next to the mapping images are the cross-sectional intensity profiles along the horizontal dashed lines. The mapping further verified that the strips corresponded to the PS domains, whereas the regions between the strips consisted of predominately PVP.

Shown in Figure 3 are the AFM images of the spin-coated blend films. In the case of the 10/90 composition, the disk shape PS domains, which lined up along the radial direction and were located at the convex region of the striations, are evidently much more elevated than the PVP surroundings. The much smaller PS disks distributed randomly between the larger PS disks and striations possess much smaller height elevations. In the case of the 30/70 composition, one observes that the thickness variation within the PS striations is much smaller than that encountered across the striations. From Figure 3a,b, the thickness variations are in the range of 200–250 nm. In this work, the film thickness is reported as the height of the film excluding the ridge portion.

The pattern of the parallel strips was indeed macroscopic, extending up to the mm length scale. It is noted that the strip

patterns were not observed near the center of the spin-cast films. There, the morphology was dominated by a cellular pattern with the discrete smaller PS domains dispersed within the cells, as shown in Figure 4a for the 30/70 PS-1/PVP blend. Slightly away from the center, a transition zone was identified from which the strip pattern of the PS phase began to appear (Figure 4b). The strips in this region were shorter and less ordered than those found in the well-developed region. Strip branching and trapped domains were also abundant here. Going further out, a well-developed region in which large-scale parallel strips formed (Figure 1d) was encountered. Since this region is of application interest, we will focus our latter discussion on the well-developed region.

**Effect of Polymer Solution Concentration.** We examined the effect of polymer solution concentration on the phase-separated morphologies of the spin-cast thin films. The film morphology was found to be strongly influenced by the polymer solution concentration. We classified the film morphology into three distinct types along the solution concentration coordinate, as shown in Figure 5. Type I morphology formed at the concentrations of 0.6–0.9%, Type II formed at 1.1–1.5%, and Type III formed at 1.7–5.0%. The well-developed periodic strip pattern was designated as the Type II morphology. The strip pattern was not well-developed in the Type I regime, where the morphology may be more appropriately described as an alternating dense and

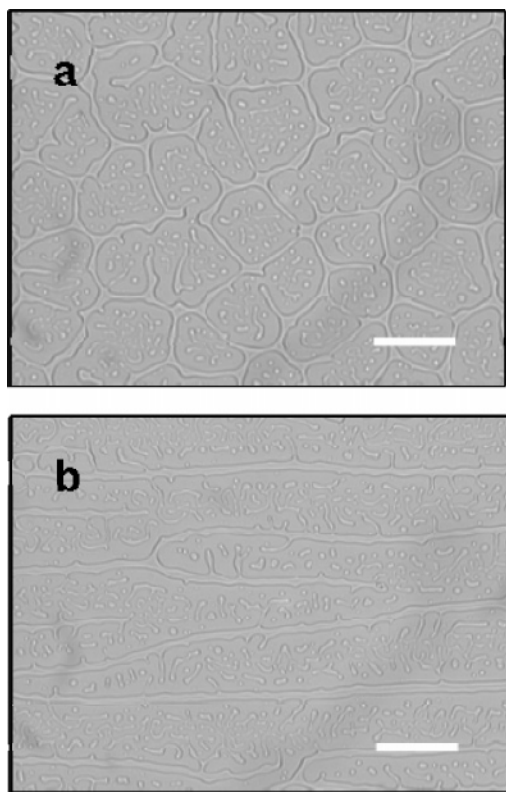


**Figure 4.** OM images of PS-1/PVP (30/70) thin films spin cast using a solution concentration of 1.3% at 6000 rpm. The images were taken from (a) the center region and (b) a transition zone next to the center region of the film, respectively. The scale bars are 50  $\mu\text{m}$  in length.

dilute PS zone pattern (Figure 5a). As for the Type III morphology, the parallel strips were severely branched and distorted (Figure 5g).

To show that the characteristic morphology was indeed long-ranged, we obtained the static laser light scattering (SLS) patterns of the samples, which gave rise to the OM images of Figure 5a,d,g, using a laser beam  $\sim 10 \text{ mm}^2$  in size. The characteristic scattering patterns from the three samples are shown in Figure 5b,e,h, respectively. Also presented in Figure 5 for comparison are the numerical fast Fourier transform (FFT) patterns of the OM images. The SLS patterns were found to agree well with the corresponding FFT patterns, indicating that the morphological structures shown in the OM images persisted to the millimeter scale. The scattering pattern associated with Type I morphology exhibited a straight line and a diffuse ring, implying the coexistence of two distinct morphological entities. The line pattern corresponded to the scattering from the strips of the thick dense PS zone, while the diffuse ring was contributed by the small PS domains isotropically dispersed within the dense and dilute PS zones (Figure 5a). In the Type II regime, the strips were well-ordered and compact; therefore, the scattering pattern was characterized by a strong line pattern and a much weaker diffuse ring, as shown in Figure 5e,f. As for the Type III morphology, the scattering pattern appeared to be an elongated diffuse ellipse. Evidently, the orientation of the strips was weakened by the severe branching and distortion, thus giving the scattering pattern of weak anisotropic features. On the basis of the morphological features depicted in Figure 5, we concluded that parallel strips were, in general, the structural feature of the blend thin films, differing only in the extent of dominance. It is, however, worth mentioning that, because of the nature of the radial morphological development, these parallel strips eventually diverge as they go further out toward the edge of the substrate.

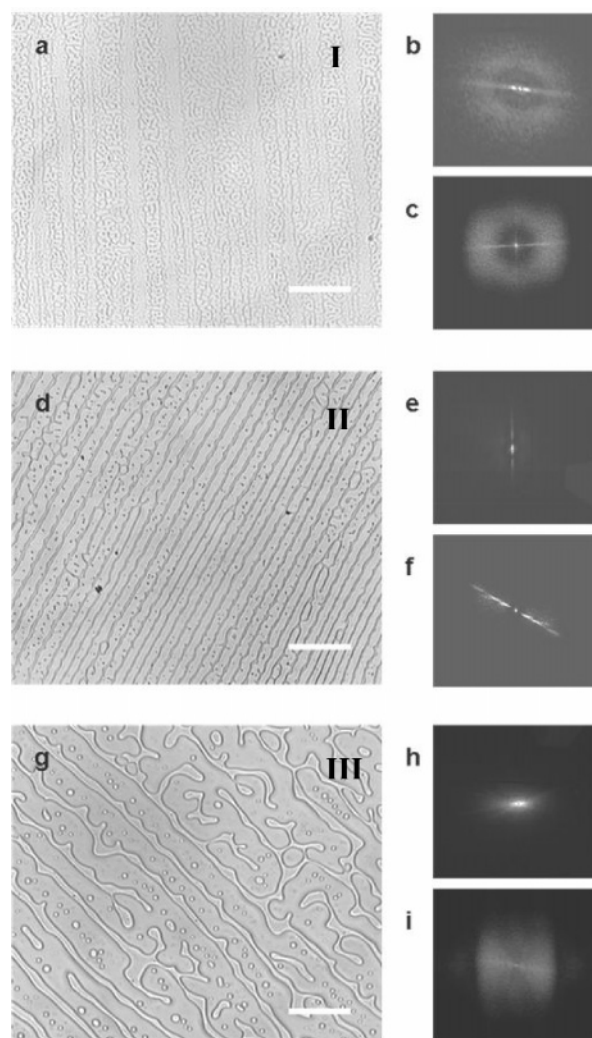


**Figure 5.** Classification of the morphological structure of the spin-cast PS-1/PVP (30/70) thin films prepared from different polymer solution concentrations. There are three distinct types of morphology: (a) Type I, prepared using 0.9% solution, (d) Type II, prepared using 1.3% solution, and (g) Type III, prepared using 2.5% solution. The corresponding SLS patterns are shown in panels b, e, and h, respectively. The corresponding two-dimensional FFT patterns are designated as panels c, f, and i, respectively. The scale bars are 100  $\mu\text{m}$  in length.

**Effect of Molecular Weight of PS.** Solution viscosity, an important factor in  $Ma$ , can be varied not only through polymer concentration but also through the molecular weights of the constituent polymers. Shown in Figure 6 is the morphology of PS-2/PVP (30/70) blend thin films cast using different solution concentrations. Here, PS-2 has a much lower molecular weight than PS-1 (Table 1). Evidently, the anisotropic self-organized patterns still remained within a larger concentration window (5–1.3% at least). This was somewhat expected since the viscosity of the PS-2/PVP solution, an important factor in  $Ma$  at the early stage of the evaporation, is lower than that of the PS-1/PVP solution, giving greater  $Ma$ . Note that the Marangoni effect is most pronounced at the early stage of the evaporation when the polymer solution is still dilute and easier to be driven to flow. As the evaporation proceeds further, the polymer solution will become increasingly too viscous to move in response to convective and/or diffusive driving forces. Interestingly, the domain geometries of the self-organized PS phases were significantly altered by the molecular weight ratio of PS to PVP. The strip

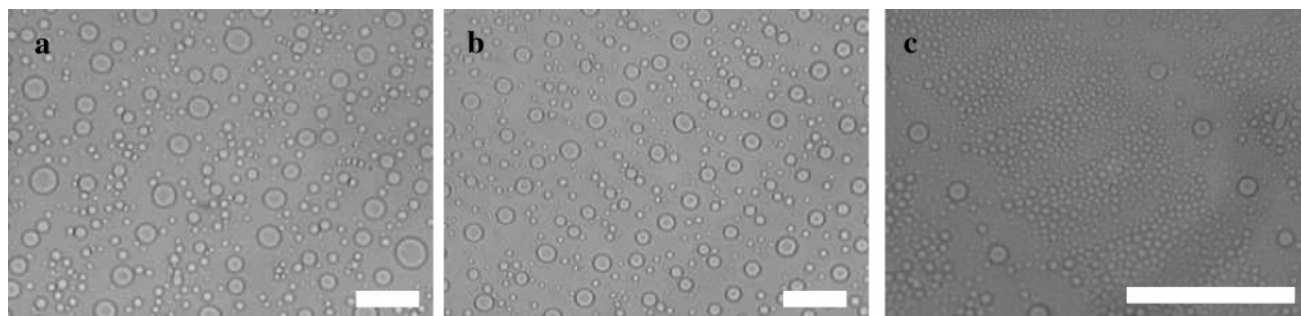


**Figure 6.** The OM images of PS-2/PVP (30/70) thin films spin cast using solution concentrations of (a) 5%, (b) 2.5%, and (c) 1.3%, at 6000 rpm. The scale bars are 50  $\mu\text{m}$  in length.

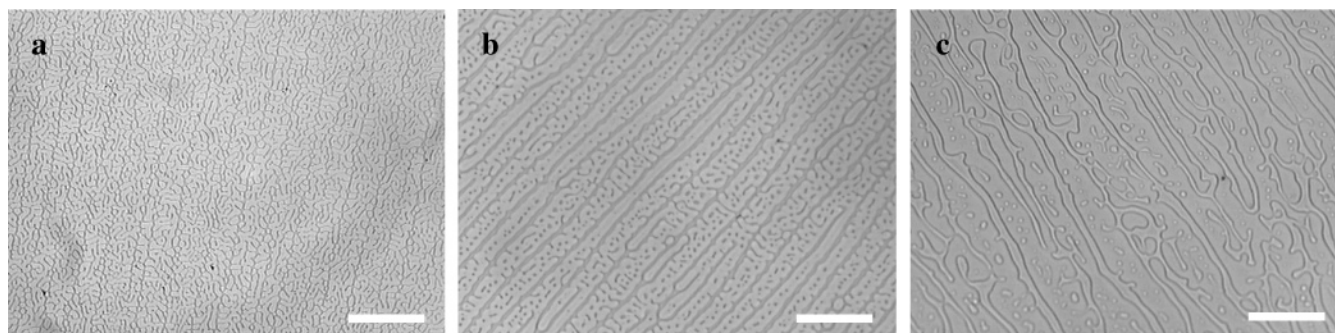


**Figure 7.** OM images of thin films of an PS-1/PVP blend spin cast on TMCS-modified glass slides at solution concentrations of (a) 0.9%, (b) 1.3%, and (c) 2.5% at 6000 rpm. The scale bars are 100  $\mu\text{m}$  in length.

patterns formed in PS-1/PVP disappeared, and only disk-shape domains in an anisotropic arrangement were observed in PS-2/PVP.

**Characterizations of Blend Thin Films Spin Cast on Hydrophobic Substrates.** To reveal the possible effect of the surface characteristics of substrates on phase-separated morphology, we further investigated the morphology of the blend films spin cast on hydrophobic surfaces (TMCS-modified substrate). The results, as depicted in Figure 7, showed that the pattern formation was not much affected by the surface characteristics of the substrate, as all basic morphological features were retained, although some deterioration in pattern regularity did occur. The Marangoni instability takes place mainly at the solution surface, and the change in surface energy is dominated by the air–polymer interface instead of the polymer–substrate interface.

**Formation Mechanism of Parallel Strip Pattern.** Here we attempt to show the connection between the formation of the strip patterns and the Marangoni effect. The magnitude of  $Ma$  is affected by a number of parameters (see eqs 1 and 2). We picked  $H^2/\mu$  to study how the Marangoni effect correlated with the morphological features since this parameter varied the most with the concentration of the starting polymer solution, which has been found in this work to play a critical role in the pattern formation of the PS/PVP blend thin films. During the spin-coating process, the viscosity of the polymer solution increased rapidly with time because of the fast solvent evaporation. In the meantime, the film experienced rapid thinning due to the interplay of centrifugal spreading and solvent evaporation. It was extremely difficult, if not impossible, to track the variations in viscosity and thickness of the spin-casting process in situ. To conduct a practically manageable, yet meaningful investigation, we took the initial viscosity of the polymer solution and the final thickness of the spin-cast films to study the effect of  $H^2/\mu$  on the magnitude of  $Ma$ . It turned out that this combination, although not a rigorous representation of  $H^2/\mu$  in  $Ma$ , did lead to rather conclusive results.

The variation of viscosity with the solution concentration is shown in Figure 8a. Below 1.7%, the viscosity increased slightly

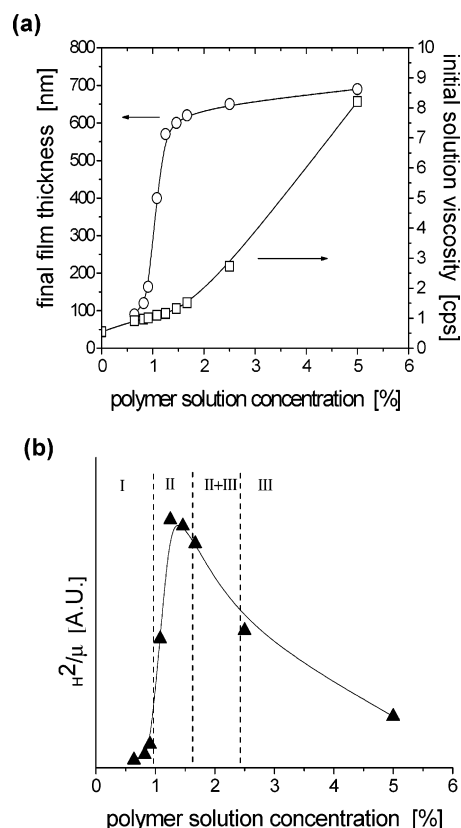


**Figure 8.** (a) The initial solution viscosity and the final film thickness versus polymer solution concentration. (b)  $H^2/\mu$  versus polymer solution concentration.

and almost linearly with the concentration. The viscosity increase became more drastic as the concentration exceeded 1.7%. On the other hand, the thickness of the spin-cast film increased rapidly with increasing concentration but then gradually leveled off above  $\sim 1\%$ . Note that the phase separation of polymer blends taking



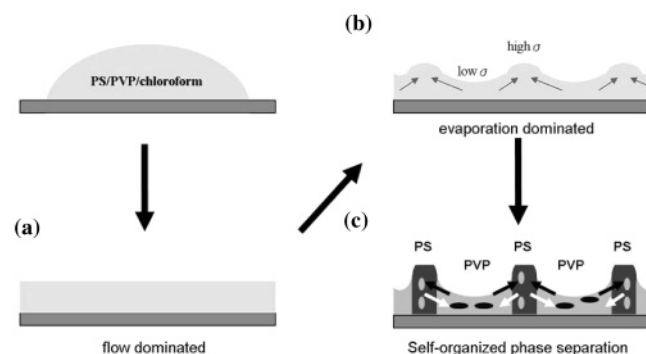


**Figure 9.** The proposed formation mechanism for periodic strip-based PS patterns within PS/PVP (30/70) spin-cast films. (a) The polymer solution layer was thinned by centrifugal spreading (flow dominated). (b) The solution layer was further thinned because of solvent evaporation (evaporation dominated), and Marangoni instability was triggered, leading to thickness variation over the surface. (c) Further evaporation induced phase separation, and the PS-rich and PVP-rich streams preferentially flowed toward the thermodynamically favored locations to smooth out the nonuniformity in surface tension.

place under the Marangoni instability resulted in large thickness variations in the range of hundreds of nanometers, as can be seen from Figure 3a,b, comparable to the film thickness. The film thickness here was defined as the height of the film excluding the ridge portion. The parameter  $H^2/\mu$ , which is relevant to Ma, was calculated and plotted as a function of concentration in Figure 8b. Interestingly,  $H^2/\mu$  reached a maximal value near a concentration of 1.3%. As shown in Figure 4, the most well-developed strip patterns, that is, Type II morphology, were also obtained near this concentration. Figure 8b was divided into four regimes, namely, I, II, major II + minor III, and III, according to Figure 5. Type II morphology was found to appear in the concentration range giving rise to greater  $H^2/\mu$  values. The good correlation between the morphological features of the ordered strip patterns and those of  $H^2/\mu$  implies that the Marangoni effect did play a major role in the formation of the strip patterns. The initial solution viscosity played an important role in the initial Marangoni instability and thus the variation pattern in *thickness* before phase separation, while the final film thickness served as a good measure for the evolution time available for the phase separation that led to the variation pattern in *composition*. Therefore, the parameter,  $H^2/\mu$ , served as a good correlation parameter for pattern regularity, and this parameter can be loosely, although not rigorously, related to the Marangoni number.

For polymer blend films cast on patterned substrates, the surface energy variation was established in advance. The constituent polymers flow to the preferential regions to achieve the lowest total interfacial energy of the system as the phase separation proceeds.<sup>25</sup> In our study, the surface energy variation was created by the Marangoni instability on the liquid–air surface. PS and PVP would flow to the suitable regions to lower the total surface energy of the system. According to the theory of Marangoni instability, as the increase in surface tension occurs at certain locations, the neighboring fluid of lower surface tension would be pulled to the high surface tension region to balance the surface tension difference. This causes a convective flow and results in mass accumulation at locations of higher surface tension. Figure 9 proposed here is one of possible mechanisms to describe the influence of Marangoni instability on the phase separation of the blend. First, the solution deposited on the substrate was thinned mainly because of centrifugal spreading, as shown in Figure 9a. Further thinning dominated by solvent evaporation then took place. Marangoni instability set in and led to the formation of

striation patterns over the solution surface, as depicted in Figure 9b. Further solvent evaporation induced the phase separation between PS and PVP. Under the influence of the Marangoni effect, the PS-rich streams of lower surface tension flowed preferentially to the ridge region, and the PVP-rich streams of higher surface tension were expelled out of the ridge region, as illustrated in Figure 9c. The polymer solution became highly viscous because of the fast solvent depletion, and the separating process of the PS and PVP phases was eventually stopped, leaving behind different extents of phase separation depending on how fast the motion of the polymers was seized. Consequently, there existed a variety of strip patterns, from alternating dense and dilute zones (Type I), to compact ordered strips (Type II), to severely branched and distorted strips (Type III).

One may argue that the viscosity difference of the two polymer solutions may play a decisive role on the pattern formation. It has been shown in the literature that, in melted-state or concentrated solutions, the polymers of low molecular weight might move independently from one another, while the movement of the polymer of high molecular weight might be retarded by more severe polymer chain entanglement.<sup>26</sup> For the present work, it was difficult to estimate the viscosities of the constituent polymers in the solutions during solvent evaporation. Nevertheless, we may use the viscosity of corresponding homopolymer solutions at a given concentration to illustrate that viscosity was not the key factor. As listed in Table 1, at a solution concentration of 1.3%, the viscosity of PS-I (2.9 cps) was larger than that of PVP (1.2 cps). Therefore, if viscosity difference plays a decisive role in the pattern formation, PVP instead of PS should have been preferentially driven to the ridge by the Marangoni convection. However, this was not what we observed. Consequently, we concluded that surface tension may be the more important factor for the pattern formation.

## Conclusions

In contrast to the previously reported thickness-varying striation pattern on spin-cast homopolymer thin films, our study showed that parallel strip patterns, manifested in both thickness and composition variations, formed via spin coating from the PS/PVP blend solutions with chloroform on unpatterned substrates. A possible mechanism was proposed to describe the formation of such regular patterns under the influence of Marangoni instability. The surface energy variation was created by the Marangoni instability on the liquid–air surface as the solvent–evaporation-induced phase separation took place during the spin-coating process. The PS-rich streams of lower surface tension were preferentially pulled toward the ridge region where the surface tension was higher initially so as to balance the surface tension difference. With high enough values of  $H^2/\mu$ , the formation of well-developed PS strips in the films was observed. This ordered morphology was also proved to be long-ranged.

**Acknowledgment.** Financial support was provided by the National Science Council of the Republic of China (NSC 94-2214-E-007-004). We acknowledge Y. C. Lee of the National Synchrotron Radiation Research Center of the Republic of China for assistance in micro-FTIR experiment and analysis.